

A NONCONFORMING IMMERSSED FINITE ELEMENT METHODS FOR ELLIPTIC INTERFACE PROBLEMS

TAO LIN [†], DONGWOO SHEEN[‡], AND XU ZHANG[§]

Abstract. A new immersed finite element (IFE) method is developed for second-order elliptic problems with discontinuous diffusion coefficient. The IFE space is constructed based on the rotated- Q_1 nonconforming finite elements with the integral-value degrees of freedom. The standard nonconforming Galerkin method is employed in this IFE method without any penalty stabilization term. Error estimates in energy- and L^2 -norms are proved to be better than $O(h\sqrt{|\log h|})$ and $O(h^2|\log h|)$, respectively, where the logarithm factors reflect jump discontinuity. Numerical results are reported to confirm our analysis.

Key words. immersed finite element, nonconforming, rotated- Q_1 , Cartesian mesh, elliptic interface problems

AMS subject classifications. 35R05, 65N15, 65N30

1. Introduction. We consider the second-order elliptic interface problem:

$$\begin{aligned} (1.1a) \quad & -\nabla \cdot (\beta \nabla u) = f \quad \text{in } \Omega^- \cup \Omega^+, \\ (1.1b) \quad & u = g \quad \text{on } \partial\Omega, \end{aligned}$$

where, without loss of generality, we assume that a C^2 -continuous interface curve Γ separates the physical domain Ω into two sub-domains Ω^+ and Ω^- , such that $\bar{\Omega} = \Omega^+ \cup \Omega^- \cup \Gamma$, see an illustration in Figure 1.1. The physical domain $\Omega \subset \mathbb{R}^2$ is assumed to be occupied by two materials such that the diffusion coefficient $\beta(x, y)$ is discontinuous across the interface Γ , and it is assumed to be a piecewise constant function defined by

$$(1.2) \quad \beta(x, y) = \begin{cases} \beta^- & \text{if } (x, y) \in \Omega^-, \\ \beta^+ & \text{if } (x, y) \in \Omega^+, \end{cases}$$

such that $\min\{\beta^-, \beta^+\} > 0$. Across the interface Γ , the solution and the normal component of the flux are assumed to be continuous, *i.e.*,

$$\begin{aligned} (1.3a) \quad & [u]_\Gamma = 0, \\ (1.3b) \quad & [[\boldsymbol{\nu} \cdot \beta \nabla u]]_\Gamma = 0, \end{aligned}$$

where $[v]_\Gamma = v^+|_\Gamma - v^-|_\Gamma$, and $[[\boldsymbol{\nu} \cdot \beta \nabla u]]_\Gamma = \boldsymbol{\nu}^+ \cdot \beta^+ \nabla u^+ + \boldsymbol{\nu}^- \cdot \beta^- \nabla u^-$, with $\boldsymbol{\nu}$ the unit normal of Γ .

Conventional finite element methods (FEM) can solve this elliptic interface problem satisfactorily provided that solution meshes are shaped to fit the material interface [4]; otherwise the accuracy of the solution is uncertain [1]. *Immersed finite element*

*This research was partially supported by the National Science Foundation Grant (DMS-1016313, DMS-1720425), NRF-2017R1A2B3012506 and NRF-2015M3C4A7065662 in part.

[†]Department of Mathematics, Virginia Tech, Blacksburg, VA 24061, tlin@math.vt.edu

[‡]Department of Mathematics, and Interdisciplinary Program in Computational Science & Technology, Seoul National University, Seoul 08826, Korea, dongwoosheen@gmail.com

[§]Department of Mathematics and Statistics, Mississippi State University, Mississippi State, MS 39762, xuzhang@math.msstate.edu

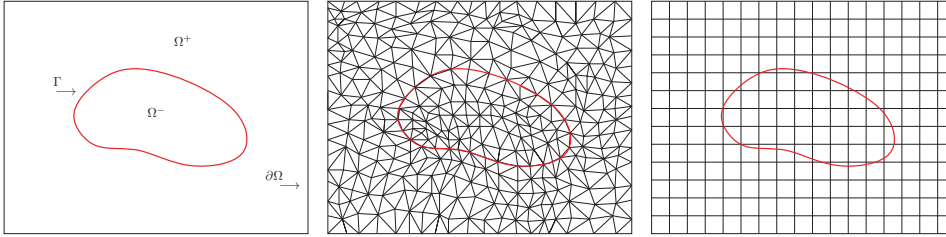


FIG. 1.1. A geometry of interface problems. Body-fitting mesh and non-body-fitting mesh.

(IFE) methods [2, 5, 10, 13, 18, 23, 24, 27, 28, 30], on the other hand, do not require meshes to fit the interface. Hence, if desired, Cartesian meshes can be used to solve interface problems which is advantageous in many simulations. For example, in particle-in-cell methods for plasma particle simulations [19, 20], it is preferable to solve the governing electric potential interface problem on Cartesian meshes for efficient particle tracking. Also, IFE methods, in either a standard fully discrete or a semi discrete (the method of lines) formulation, can be used to solve time dependent problems with moving interfaces [16, 25] on a fixed Cartesian mesh throughout the whole simulation.

The basic idea of IFE methods is to locally modify finite element functions on interface elements to fit the interface jump conditions (1.3a) and (1.3b). For elliptic interface problems, most IFE methods in the literature are modified from the Lagrange type conforming finite element spaces, whose degrees of freedom are determined by nodal values at the mesh points. However, IFE spaces originated from these conforming FE spaces are usually nonconforming because IFE functions are discontinuous across interface edges. This discontinuity can be harmfully large for certain configuration of interface location and diffusion coefficient. Consequently, the IFE solution is often less accurate around the interface than the rest of solution domain. Our recent study in [26, 31] indicates that the convergence rates of these conforming type IFE functions used in the Galerkin formulation can deteriorate as the mesh size gets small.

New *partially penalized immersed finite element* (PPIFE) methods are recently introduced in [26, 31] to cope with the negative impacts caused by the discontinuity in IFE functions. In the new PPIFE scheme, the flux jump terms and penalty terms are added on the interface edges to ensure the consistency and the stability of the scheme. These PPIFE methods significantly improve the numerical approximation as the errors around the interface are reduced dramatically, and overall convergence rates are very stable in both energy and the L^2 - norms. Moreover, it is theoretically proved that the PPIFE methods convergence optimally in energy norm provided that the exact solution is piecewise smooth [26].

In this article, we develop a new IFE method that uses an alternative approach to effectively alleviate the harmful impacts of discontinuity in IFE functions. In this new framework, the continuity of each IFE function across element boundary is weakly enforced; hence there is *no need to add penalty terms in the new scheme*. Specifically, the new IFE space is based on nonconforming finite element spaces [3, 7, 8, 21, 29] rather than conforming Lagrange type finite element spaces. One significant difference between conforming and nonconforming finite elements is the way to impose the continuity of finite element functions across elements. Conforming FE functions

enforce continuity through nodal values at mesh points, while the continuity of non-conforming FE functions is imposed weakly through average values over edges. For IFE methods, an interface edge is cut by the interface into two pieces. The restriction of an IFE function to an interface edge leads to two piecewise polynomials from the two adjacent interface elements sharing this edge. In the conforming finite element framework, these two piecewise polynomials coincide at the two endpoints of the interface edge, and this guarantees the continuity of the IFE function at the end nodes of the interface edge but not the whole interface edge. On the other hand, in the nonconforming framework, the continuity across an element edge is weakly enforced over the whole edge in the integral sense, no matter whether it is a polynomial or a piecewise polynomial. Thus we can take advantage of this nonconforming mechanism for constructing IFE functions that weakly preserve continuity over the whole of each interface edge.

The simplest nonconforming finite element defined on triangular meshes is the well-known Crouzeix-Raviart element [7]. For rectangular meshes, the simplest nonconforming finite elements are known as the *rotated- Q_1 finite elements* [3, 8, 21, 29]. Their degrees of freedom are determined either by values at midpoints of edges or by the integral values over edges. These two types of degrees of freedom define two different finite element spaces if the basis functions are taken as in [29], but an identical space if the basis functions are taken as in [3, 17]. The Crouzeix-Raviart type IFE method was discussed in [22]. In this article, we develop a new IFE space based on the rotated- Q_1 functions with the integral-value degrees of freedom. We will derive quasi-optimal error estimates in both energy and L^2 - norms for the simple Galerkin approximation. In our error analysis, we extend a special projection operator introduced in [8] to bound the flux error on edges. We show that the flux error on interface edges will have a $\log |h|$ factor. The techniques in our error analysis are new to interface problems and they are different from analysis in literature such as [22].

The rest of this article is organized as follows. In Section 2, we present nonconforming rotated- Q_1 IFE space and present some basic properties. In Section 3, we discuss the approximation capabilities of the IFE space. In Section 4, we analyze errors of Galerkin solutions to the elliptic interface problem in energy and L^2 norms. In Section 5, numerical results are presented to confirm our analysis and to demonstrate features of the new IFE method. Finally, a few brief conclusions are provided in Section 6.

2. Nonconforming Immersed Finite Element Space. This section starts with notations and some preliminaries to be used in this paper. Then, we will introduce the IFE space based on nonconforming rotated- Q_1 elements.

2.1. Notations and Preliminaries. Multi-index notations will be employed such that $\alpha = (\alpha_1, \alpha_2) \in [\mathbb{Z}^+]^2$, $|\alpha| = \alpha_1 + \alpha_2$, together with the partial differential operator $\partial^\alpha = \frac{\partial^{\alpha_1}}{\partial x_1^{\alpha_1}} \frac{\partial^{\alpha_2}}{\partial x_2^{\alpha_2}}$, where \mathbb{Z}^+ denotes the set of all nonnegative integers. By \tilde{S} we denote the union of finite number of mutually disjoint open sets $S_j \subset \mathbb{R}^2$, $j = 1, \dots, J$, and by S the interior of \tilde{S} , which contains \tilde{S} and all its possible interfaces. If $J = 1$, $\tilde{S} = S$. Let $W^{m,p}(\tilde{S})$ denote the usual Sobolev space with non-negative integer index m , equipped the norm and seminorm:

$$\|v\|_{m,p,\tilde{S}} = \left(\sum_{|\alpha| \leq m} \int_{\tilde{S}} |\partial^\alpha v(\mathbf{x})|^p \, dx \right)^{1/p}, \quad |v|_{m,p,\tilde{S}} = \left(\sum_{|\alpha|=m} \int_{\tilde{S}} |\partial^\alpha v(\mathbf{x})|^p \, dx \right)^{1/p},$$

for $1 \leq p < \infty$, and

$$\|v\|_{m,\infty,\tilde{S}} = \max_{|\alpha| \leq m} \text{ess.sup}\{|v(x)| : x \in \tilde{S}\}, \quad |v|_{m,\infty,\tilde{S}} = \max_{|\alpha|=m} \text{ess.sup}\{|v(x)| : x \in \tilde{S}\}.$$

In particular, for $p = 2$, we denote $H^m(\tilde{S}) = W^{m,p}(\tilde{S})$, and we omit the index p in associated norms and seminorms for simplicity, *i.e.*, $\|v\|_{m,2,\tilde{S}} = \|v\|_{m,\tilde{S}}$, and $|v|_{m,2,\tilde{S}} = |v|_{m,\tilde{S}}$. We will also follow the convention to drop the domain index \tilde{S} if $\tilde{S} = \Omega$. For $p = 2$, associated with the norm $\|\cdot\|_{m,\tilde{S}}$, the inner product for $H^m(\tilde{S})$ will be denoted by $(\cdot, \cdot)_{H^m(\tilde{S})}$, with further simplification to $(\cdot, \cdot)_{\tilde{S}}$ and (\cdot, \cdot) if $m = 0$ and also if $\tilde{S} = \Omega$, respectively.

For $m \geq 1$, we define two types of subspaces of $H^m(\tilde{S})$ whose functions satisfy the interface jump conditions (1.3a) and (1.3b) on Γ . First, we set

$$\tilde{H}_\Gamma^m(S) = H^1(S) \cap H^m(\tilde{S}),$$

endowed with the inner-product and the norm

$$\langle u, v \rangle_{\tilde{H}_\Gamma^m(S)} = (u, v)_{H^1(S)} + \sum_{j=1}^J \sum_{|\alpha|=2}^m (\partial^\alpha u, \partial^\alpha v)_{L^2(S^j)}, \quad \|u\|_{\tilde{H}_\Gamma^m(S)} = \sqrt{\langle u, u \rangle_{\tilde{H}_\Gamma^m(S)}}.$$

Notice that $\tilde{H}_\Gamma^1(S) = H^1(S)$ and that

$$[v]_\Gamma = 0 \text{ in the sense of } H^{\frac{1}{2}}(\Gamma) \quad \forall v \in \tilde{H}_\Gamma^m(S), \quad m \geq 1.$$

Finally, for $m = 2$, we define a subspace of $\tilde{H}_\Gamma^m(S)$, which will be suitable for the analysis of interface problem, as follows:

$$\tilde{H}_\beta^2(S) = \left\{ v \in \tilde{H}_\Gamma^2(S) : \llbracket \boldsymbol{\nu}_\Gamma \cdot \beta \nabla v \rrbracket_\Gamma = 0 \right\}.$$

In addition, the following spaces will be useful: for $p \geq 2$,

$$\tilde{W}_\Gamma^{2,p}(S) = W^{1,p}(S) \cap W^{2,p}(\tilde{S}); \quad \tilde{W}_\beta^{2,p}(S) = \{v \in \tilde{W}_\beta^{2,p}(\Omega) \mid \llbracket \boldsymbol{\nu}_\Gamma \cdot \beta \nabla v \rrbracket_\Gamma = 0\}.$$

Here, and in what follows, $[v]_\Gamma$ and $\llbracket v \rrbracket_\Gamma$ will mean the jumps across Γ in the sense of $W^{1-\frac{1}{p},p}(\Gamma)$ and $W^{-\frac{1}{p},p}(\Gamma)$, respectively. However, if $u \in W^{2,p}(\tilde{S})$, these jumps are defined in the sense of $W^{2-\frac{1}{p},p}(\Gamma)$ and $W^{1-\frac{1}{p},p}(\Gamma)$, respectively.

Assume that $f \in H^{-1}(\Omega)$, where $H^{-1}(\Omega)$ is the dual space of $H_0^1(\Omega) = \tilde{H}_{\Gamma,0}^1(\tilde{\Omega})$. For the interface problem described by (1.1) and (1.3), we consider its weak form: find $u \in H^1(\Omega)$ such that $u = g$ on $\partial\Omega$ and

$$(2.1) \quad a(u, v) = L(v) \quad \forall v \in H_0^1(\Omega),$$

where

$$a(u, v) = (\beta \nabla u, \nabla v), \quad L(v) = \langle f, v \rangle_{H^{-1}(\Omega), H_0^1(\Omega)},$$

$\langle \cdot, \cdot \rangle_{V', V}$ being the duality pairing between the topological vector space V and its dual space V' . An application of the Lax-Milgram Lemma shows that there exists a unique solution $u \in H^1(\Omega)$ for (2.1) such that

$$\|u\|_1 \leq C \|f\|_{-1},$$

where C is a positive constant depending only on Ω and β .

2.2. Nonconforming FE functions. Let Ω be a rectangular domain or a union of rectangular domains. Without loss of generality, assume that $\{\mathcal{T}_h\}$ is a family of uniform Cartesian meshes for domain Ω with mesh parameter $h > 0$. For each element $T \in \mathcal{T}_h$, we call it an interface element if the interior of T intersects with the interface Γ ; otherwise, we call it a non-interface element. Without loss of generality, we assume that interface elements in \mathcal{T}_h satisfy the following hypotheses when the mesh size h is small enough:

- (H1) The interface Γ cannot intersect an edge of any rectangular element at more than two points unless the edge is part of Γ .
- (H2) The interface Γ can only intersect the boundary of an interface element at two points, and these intersection points must be on different edges of this element.

Denote by \mathcal{T}_h^i and $\mathcal{T}_h^n = \mathcal{T}_h \setminus \mathcal{T}_h^i$ the collections of all interface elements and non-interface elements, respectively. For a typical rectangular element $T = \square A_1 A_2 A_3 A_4 \in \mathcal{T}_h$, the following conventions for its vertices and edges are assumed:

$$(2.2) \quad A_1 = (x_0, y_0), \quad A_2 = (x_0 + h_x, y_0), \quad A_3 = (x_0 + h_x, y_0 + h_y), \quad A_4(x_0, y_0 + h_y),$$

and

$$(2.3) \quad \gamma_1 = \overline{A_1 A_2}, \quad \gamma_2 = \overline{A_2 A_3}, \quad \gamma_3 = \overline{A_3 A_4}, \quad \gamma_4 = \overline{A_4 A_1}.$$

We follow the classical triplet definition of a finite element [6]. On the element T , the local FE space is defined by

$$(2.4) \quad \Pi_T = \text{Span} \left\{ 1, \frac{x - x_0}{h_x}, \frac{y - y_0}{h_y}, \left(\frac{x - x_0}{h_x} \right)^2 - \left(\frac{y - y_0}{h_y} \right)^2 \right\}.$$

The degrees of freedom are defined as the average values over edges:

$$(2.5) \quad \Sigma_T = \left\{ \frac{1}{|\gamma_j|} \int_{\gamma_j} \psi_T \, ds, j = 1, 2, 3, 4 : \forall \psi \in \Pi_T \right\},$$

where $|\gamma_j|$ denotes the length of the edge γ_j . The local basis functions $\psi_{j,T}$, $j = 1, 2, 3, 4$, fulfill

$$(2.6) \quad \frac{1}{|\gamma_k|} \int_{\gamma_k} \psi_{j,T} \, ds = \delta_{jk}, \quad \forall j, k = 1, 2, 3, 4.$$

Set the local finite element space on an element T as follows

$$(2.7) \quad S_h^n(T) = \text{Span} \{ \psi_{j,T} : j = 1, 2, 3, 4 \}.$$

It is obvious that on every element $T \in \mathcal{T}_h$, $S_h^n(T) = \Pi_T$.

2.3. Nonconforming IFE Functions. Next, we describe the construction of a local IFE function ϕ_T on a typical interface element $T \in \mathcal{T}_h^i$ whose vertices and edges are given in (2.2) - (2.3).

Assume that an interface curve Γ intersects $T \in \mathcal{T}_h^i$ at two different points D and E , and the line segment \overline{DE} separates T into two subelements T^+ and T^- . Depending on the adjacency of the edges containing D and E , the interface elements will be classified as Type I and Type II interface elements such that these two edges

are located at two adjacent edges and at two opposite edges, respectively. We use a Type II interface element to exemplify the construction of the local IFE functions and corresponding spaces, i.e., we assume the interface points are such that

$$D = (x_0 + dh_x, y_0), \quad E = (x_0 + eh_x, y_0 + h_y),$$

where $d, e \in (0, 1)$. The local IFE function ϕ_T is defined as a piecewise rotated Q_1 polynomial as follows:

$$(2.8) \quad \phi_T(x, y) = \begin{cases} c_1^+ + c_2^+ \left(\frac{x - x_0}{h_x} \right) + c_3^+ \left(\frac{y - y_0}{h_y} \right) + c_4^+ \left(\left(\frac{x - x_0}{h_x} \right)^2 - \left(\frac{y - y_0}{h_y} \right)^2 \right) & \text{in } T^+, \\ c_1^- + c_2^- \left(\frac{x - x_0}{h_x} \right) + c_3^- \left(\frac{y - y_0}{h_y} \right) + c_4^- \left(\left(\frac{x - x_0}{h_x} \right)^2 - \left(\frac{y - y_0}{h_y} \right)^2 \right) & \text{in } T^-. \end{cases}$$

The coefficients c_j^\pm are determined by the average value v_j on each edge γ_j :

$$(2.9) \quad \frac{1}{|\gamma_j|} \int_{\gamma_j} \phi_T \, ds = v_j, \quad j = 1, 2, 3, 4,$$

and the following interface jump conditions

$$(2.10) \quad [\phi_T]_{\overline{DE}} = 0,$$

and

$$(2.11) \quad \int_{\overline{DE}} [\boldsymbol{\nu}_{\overline{DE}} \cdot \beta \nabla \phi_T]_{\overline{DE}} \, ds = 0,$$

where $\boldsymbol{\nu}_{\overline{DE}}$ is the unit normal on \overline{DE} . Note that the continuity condition (2.10) is equivalent to

$$(2.12) \quad [\phi_T(D)] = 0, \quad [\phi_T(E)] = 0, \quad c_4^+ = c_4^-.$$

Equations (2.9)–(2.11) provide eight constraints and lead to an 8×8 algebraic system $M_c \mathbf{C} = \mathbf{V}$ about the coefficients $\mathbf{C} = (c_1^-, \dots, c_4^-, c_1^+, \dots, c_4^+)^t$ with $\mathbf{V} = (v_1, \dots, v_4, 0, \dots, 0)^t$. By direct calculations, one can verify that the matrix M_c is nonsingular for all $\beta^\pm > 0$ and $0 < d, e < 1$; see [31] for more details. Hence, an IFE function ϕ_T satisfying jump conditions (2.10) and (2.11) is uniquely determined by its integral values v_j over edges γ_j , $j = 1, 2, 3, 4$. For each $j = 1, 2, 3, 4$, let $\mathbf{V} = \mathbf{V}_j = (v_1, \dots, v_4, 0, \dots, 0)^t \in \mathbb{R}^8$ be the j -th canonical vector such that $v_j = 1$ and $v_k = 0$ for $k \neq j$. We can solve for $\mathbf{C}_j = (c_1^-, \dots, c_4^-, c_1^+, \dots, c_4^+)^t$ and use it in (2.8) to form the j -th nonconforming rotated- Q_1 local IFE basis function $\phi_{j,T}$. Figure 2.1 presents illustrations for a comparison of a standard rotated Q_1 finite element basis function and its corresponding rotated Q_1 IFE basis functions in both Type I and Type II interface elements.

Denote by $S_h^i(T) = \text{Span} \{ \phi_{j,T} : j = 1, 2, 3, 4 \}$ the local rotated- Q_1 IFE space on an interface element T . The global IFE space is defined as follows

$$(2.13) \quad S_h(\Omega) = \left\{ v \in L^2(\Omega) : v|_T \in S_h^n(T) \text{ if } T \in \mathcal{T}_h^n, v|_T \in S_h^i(T) \text{ if } T \in \mathcal{T}_h^i; \int_\gamma [v]_\gamma \, ds = 0 \text{ for all interior edges } \gamma \text{ of } \mathcal{T}_h \right\}.$$

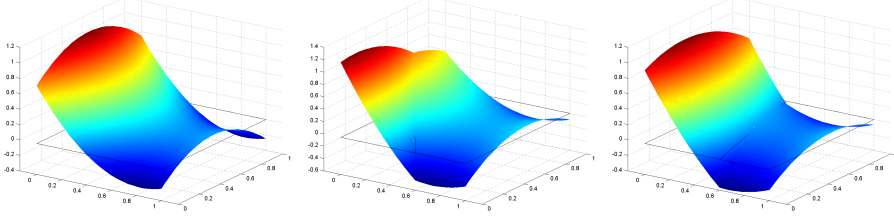


FIG. 2.1. Nonconforming FE/IFE local bases with integral-value degrees of freedom

2.4. Basic Properties of IFE Space. We summarize some basic and useful properties for the IFE space $S_h(\Omega)$ in this subsection. The results can be verified via straightforward calculation, and we also refer to [31] for some of their proofs.

LEMMA 2.1. (**Unisolvency**) *On each interface element $T \in \mathcal{T}_h^i$, an IFE function $\phi_T \in S_h^i(T)$ is uniquely determined by its integral values (2.9) and interface jump conditions (2.10) and (2.11).*

LEMMA 2.2. (**Continuity**) *On each interface element $T \in \mathcal{T}_h^i$, the local IFE space $S_h^i(T) \subset C^0(T)$.*

LEMMA 2.3. (**Partition of Unity**) *On each interface element $T \in \mathcal{T}_h^i$, the IFE basis functions $\phi_{i,T}$ satisfy the partition of unity property, i.e.,*

$$(2.14) \quad \sum_{j=1}^4 \phi_{j,T}(x, y) = 1, \quad \forall (x, y) \in T.$$

LEMMA 2.4. (**Consistency**) *On each interface element $T \in \mathcal{T}_h^i$, the IFE basis functions are consistent to standard finite element basis functions in the following sense:*

1. *If there is no jump in the coefficient, i.e., $\beta^+ = \beta^-$, then the IFE basis functions $\phi_{j,T}$ become the standard FE basis functions $\psi_{j,T}$.*
2. *If $\min\{|T^+|, |T^-|\}$ shrinks to zero, then the IFE basis functions $\phi_{j,T}$ become the standard FE basis functions $\psi_{j,T}$. Here, $|T^s|$ denotes the area of T^s , $s = +, -$.*

LEMMA 2.5. (**Flux continuity on Γ**) *On each interface element $T \in \mathcal{T}_h^i$, every IFE function $\phi_T \in S_h^i(T)$ satisfies the flux jump condition weakly as follows*

$$\int_{\Gamma \cap T} [[\boldsymbol{\nu} \cdot \beta \nabla \phi_T]]_{\Gamma \cap T} ds = 0,$$

where $\boldsymbol{\nu}$ is the unit normal to Γ .

LEMMA 2.6. (**Boundedness**) *There exists a constant C , independent of interface location, such that for $j = 1, 2, 3, 4$, and $k = 0, 1, 2$,*

$$(2.15) \quad \|\phi_{j,T}\|_{k,\infty,T} \leq Ch^{-k} \quad \forall T \in \mathcal{T}_h^i.$$

THEOREM 2.7. (**Trace Inequality**) *There exists a constant $C > 0$, depending only on the diffusion coefficient β , such that*

$$(2.16) \quad \|\boldsymbol{\nu} \cdot \beta \nabla v\|_{0,\gamma} \leq Ch_T^{-\frac{1}{2}} \|\nabla v\|_{0,T} \quad \forall v \in S_h^i(T)$$

where γ is an edge of T , and $\boldsymbol{\nu}$ is the unit outward normal to T .

THEOREM 2.8. (Inverse Inequality) *There exists a constant C , depending only on the diffusion coefficient β , such that*

$$(2.17) \quad |v|_{k,\infty,T} \leq Ch_T^{-1}|v|_{k,T}, \quad |v|_{k,T} \leq Ch_T^{l-k}|v|_{l,T}, \quad \forall v \in S_h^i(T), \quad 0 \leq l \leq k \leq 2.$$

3. The Interpolation Operator and Approximation Capability. In this section, we discuss the approximation capability for the nonconforming IFE space $S_h(\Omega)$. On each non-interface element $T \in \mathcal{T}_h^n$, the local interpolation is defined canonically by $\mathcal{I}_T : C(\bar{T}) \rightarrow S_h^n(T)$, such that,

$$(3.1) \quad \mathcal{I}_T u = \sum_{i=1}^4 \left(\frac{1}{|\gamma_i|} \int_{\gamma_i} u \, ds \right) \psi_{i,T},$$

where γ_j denote the edges of T . The standard scaling argument leads to the following error estimates [29, Lemma 1]:

$$(3.2) \quad \|\mathcal{I}_T u - u\|_{0,T} + h|\mathcal{I}_T u - u|_{1,T} \leq Ch^2|u|_{2,T}.$$

On each interface element $T \in \mathcal{T}_h^i$, the interpolation operator $\mathcal{I}_T : C(\bar{T}) \rightarrow S_h^i(T)$ is defined similarly as follows:

$$(3.3) \quad \mathcal{I}_T u = \sum_{i=1}^4 \left(\frac{1}{|\gamma_i|} \int_{\gamma_i} u \, ds \right) \phi_{i,T} \quad \forall u \in C(\bar{T}).$$

Finally, we define the global IFE interpolation $\mathcal{I}_h : C(\bar{\Omega}) \rightarrow S_h(\Omega)$ piecewisely such that

$$(\mathcal{I}_h u)|_T = \mathcal{I}_T u \quad \forall T \in \mathcal{T}_h.$$

The error estimates for the interpolation operator on interface elements are reported in [11, 12, 31]. We only state the results in the following theorems.

THEOREM 3.1. *There exists a constant $C > 0$, independent of interface location, such that*

$$(3.4) \quad \|\mathcal{I}_T u - u\|_{0,T} + h|\mathcal{I}_T u - u|_{1,T} \leq Ch^2 \|u\|_{\tilde{H}_\beta^2(T)} \quad \forall u \in \tilde{H}_\beta^2(T),$$

on interface element $T \in \mathcal{T}_h^i$.

THEOREM 3.2. *There exists a constant $C > 0$, such that the following interpolation error estimate holds:*

$$(3.5) \quad \|\mathcal{I}_h u - u\|_{0,\Omega} + h \left(\sum_{T \in \mathcal{T}_h} |\mathcal{I}_T u - u|_{1,T}^2 \right)^{\frac{1}{2}} \leq Ch^2 \|u\|_{\tilde{H}_\beta^2(\Omega)} \quad \forall u \in \tilde{H}_\beta^2(\Omega).$$

4. The IFE Galerkin Method and Error Estimates. In this section, we consider a nonconforming IFE Galerkin method and carry out its error estimation.

4.1. The nonconforming IFE Galerkin method. Given a mesh \mathcal{T}_h , we denote by \mathcal{E}_h , $\mathring{\mathcal{E}}_h$ and \mathcal{E}_h^b the set of its edges, interior edges, and boundary edges, respectively. The sets of interface edges and non-interface edges are denoted by \mathcal{E}_h^i and \mathcal{E}_h^n , respectively. For the sake of simplicity, in the following discussion, we assume that the interface curve Γ does not intersect the boundary $\partial\Omega$. Consequently, $\mathcal{E}_h^b \subset \mathcal{E}_h^n$.

Define the bilinear and linear form

$$a_h(u, v) = \sum_{T \in \mathcal{T}_h} \int_T \beta \nabla u \cdot \nabla v \, dx, \quad L(v) = \sum_{T \in \mathcal{T}_h} \int_T f v \, dx.$$

The nonconforming IFE Galerkin method is to find $u_h \in S_h(\Omega)$ such that

$$(4.1) \quad a_h(u_h, v_h) = L(v_h), \quad \forall v_h \in \mathring{S}_h(\Omega),$$

subject to the boundary conditions:

$$(4.2) \quad \int_{\gamma} u_h \, ds = \int_{\gamma} g \, ds, \quad \forall \gamma \in \mathcal{E}_h^b,$$

and the test function space is defined as follows

$$\mathring{S}_h(\Omega) = \{v \in S_h(\Omega) : \int_{\gamma} v \, ds = 0, \text{ if } \gamma \in \mathcal{E}_h^b\}.$$

In the following, we derive the error estimation of IFE solution u_h .

4.2. Projection operators. For convenience in the analysis to follow, let

$$\gamma_{jk} = \partial T_j \cap \partial T_k, \quad \gamma_j = \partial T_j \cap \partial \Omega, \quad \forall T_j, T_k \in \mathcal{T}_h,$$

and write

$$v_j = v|_{T_j} \quad \forall T_j \in \mathcal{T}_h; \quad v_{jk} = v_j|_{\gamma_{jk}} \quad \forall \gamma_{jk} \in \mathcal{E}_h^i.$$

Set

$$\Lambda^h = \left\{ \lambda \mid \lambda = (\lambda_{jk}, \lambda_{kj}) \in (\mathcal{P}_0(\gamma_{jk}))^2, \lambda_{jk} + \lambda_{kj} = 0 \quad \forall \gamma_{jk} \in \mathring{\mathcal{E}}_h; \right. \\ \left. \lambda = \lambda_j \in \mathcal{P}_0(\gamma_j) \quad \forall \gamma_j \in \mathcal{E}_h^b \right\}.$$

Denote by $\boldsymbol{\nu}_j$ the unit outward normal to T_j . We will use the following projection operators introduced in [8]: $\Pi_0 : \prod_{\gamma \in \mathcal{E}_h} L^2(\gamma) \rightarrow \prod_{\gamma \in \mathcal{E}_h} \mathcal{P}_0(\gamma)$ and $\Pi_{\boldsymbol{\nu}} : \tilde{H}_{\beta}^2(\Omega) \rightarrow \Lambda^h$ by

$$(4.3) \quad \langle v - \Pi_0 v, 1 \rangle_{\gamma} = 0 \quad \forall v \in L^2(\gamma) \quad \forall \gamma \in \mathcal{E}_h,$$

$$(4.4) \quad \left\langle \beta \frac{\partial v_j}{\partial \boldsymbol{\nu}_j} - \Pi_{\boldsymbol{\nu}} v, 1 \right\rangle_{\gamma_{jk}} = 0 \quad \forall v \in \tilde{H}_{\beta}^2(\Omega) \quad \forall \gamma_{jk} \in \mathcal{E}_h,$$

so that $\Pi_0^{\gamma}(v) := \Pi_0(v|_{\gamma}) = \frac{1}{|\gamma|} \int_{\gamma} v \, ds$ is the average of v over γ and

$$(\Pi_{\boldsymbol{\nu}} v|_{\gamma_{jk}}, \Pi_{\boldsymbol{\nu}} v|_{\gamma_{kj}}) = \left(\Pi_0^{\gamma_{jk}} \beta \frac{\partial v_j}{\partial \boldsymbol{\nu}_j}, \Pi_0^{\gamma_{kj}} \beta \frac{\partial v_k}{\partial \boldsymbol{\nu}_k} \right) \in \mathbb{R}^2 \quad \forall \gamma_{jk} \in \mathcal{E}_h^i.$$

LEMMA 4.1. Let $\gamma = (0, h)$ with $\gamma^- = (0, \alpha)$ and $\gamma^+ = (\alpha, h)$. Assume $u \in L^2(\gamma)$ and $u|_{\gamma^s} \in H^{\frac{1}{2}}(\gamma^s)$, $s = -, +$. Then $u \in H^{\frac{1}{2}-\epsilon}(\gamma)$ for every $\epsilon \in (0, \frac{1}{4})$, and there exists a constant C such that

$$\|u\|_{\frac{1}{2}-\epsilon, \gamma} \leq \frac{C}{\sqrt{\epsilon}} \left(\|u\|_{\frac{1}{2}, \gamma^-} + \|u\|_{\frac{1}{2}, \gamma^+} \right).$$

Proof. For every $\epsilon \in (0, \frac{1}{4})$, let $\sigma = \frac{1}{2} - \epsilon$. Then $\sigma \in (\frac{1}{4}, \frac{1}{2})$. For $q \geq 1$ and $y \in \gamma^-$,

$$\int_{\gamma^+} \frac{1}{|x-y|^{(1+2\sigma)q}} dx = \frac{(h-y)^{1-(1+2\sigma)q} - (\alpha-y)^{1-(1+2\sigma)q}}{1-(1+2\sigma)q}.$$

Since $\sigma \in (\frac{1}{4}, \frac{1}{2})$, we specifically choose

$$q = \frac{1}{2} \left(1 + \frac{2}{1+2\sigma} \right) \implies q = \frac{2-\epsilon}{2(1-\epsilon)}.$$

Then $1 \leq q < \frac{2}{1+2\sigma}$, $1 - (1+2\sigma)q \neq -1$, and $1+2\sigma \leq (1+2\sigma)q < 2$. Hence,

$$\begin{aligned} I(\gamma^-, \gamma^+, \sigma, q) &:= \int_{\gamma^-} \int_{\gamma^+} \frac{1}{|x-y|^{(1+2\sigma)q}} dx dy \\ &= \left(\frac{1}{1-(1+2\sigma)q} \right) \left(\frac{1}{2-(1+2\sigma)q} \right) \left(h^{2-(1+2\sigma)q} - (h-\alpha)^{2-(1+2\sigma)q} - \alpha^{2-(1+2\sigma)q} \right) \\ &\leq C \left| \frac{1}{1-(1+2\sigma)q} \right| \left| \frac{1}{2-(1+2\sigma)q} \right| = C \left| \frac{1}{1-\epsilon} \right| \left| \frac{1}{\epsilon} \right| \leq \frac{C}{\epsilon}. \end{aligned}$$

Therefore, using p such that $\frac{1}{p} + \frac{1}{q} = 1$, and the above estimate, we have

$$\begin{aligned} &\int_{\gamma^-} \int_{\gamma^+} \frac{|u(x) - u(y)|^2}{|x-y|^{1+2\sigma}} dx dy \\ &\leq \int_{\gamma^-} \left(\left[\int_{\gamma^+} |u(x) - u(y)|^{2p} dx \right]^{\frac{1}{2p}} \right)^2 \left[\int_{\gamma^+} \frac{1}{|x-y|^{(1+2\sigma)q}} dx \right]^{\frac{1}{q}} dy \\ &\leq 2 \int_{\gamma^-} \|u\|_{0,2p,\gamma^+}^2 \left[\int_{\gamma^+} \frac{1}{|x-y|^{(1+2\sigma)q}} dx \right]^{\frac{1}{q}} dy + 2 \int_{\gamma^-} |u(y)|^2 \left[\int_{\gamma^+} \frac{1}{|x-y|^{(1+2\sigma)q}} dx \right]^{\frac{1}{q}} dy. \\ &\leq 2 \|u\|_{0,2p,\gamma^+}^2 \left(\int_{\gamma^-} 1^p dy \right)^{\frac{1}{p}} I(\gamma^-, \gamma^+, \sigma, q)^{\frac{1}{q}} + 2 \left(\int_{\gamma^-} |u(y)|^{2p} dy \right)^{\frac{1}{p}} I(\gamma^-, \gamma^+, \sigma, q)^{\frac{1}{q}} \\ &\leq C \|u\|_{0,2p,\gamma^+}^2 \left(\frac{1}{\epsilon} \right)^{\frac{1}{q}} + C \|u\|_{0,2p,\gamma^-}^2 \left(\frac{1}{\epsilon} \right)^{\frac{1}{q}} \\ &\leq C \left(\frac{1}{\epsilon} \right)^{\frac{2(1-\epsilon)}{2-\epsilon}} \left(\|u\|_{\frac{1}{2}, \gamma^-}^2 + \|u\|_{\frac{1}{2}, \gamma^+}^2 \right). \end{aligned}$$

In the last step, we used the Sobolev embedding theorem for one dimension:

$$W^{\frac{1}{2},2}(\gamma^s) \hookrightarrow W^{0,p}(\overline{\gamma^s}), \quad s = -, +, \quad p \in [1, \infty).$$

By definition of the fractional Sobolev norm, we have

$$\begin{aligned}
\|u\|_{\sigma,\gamma}^2 &= \|u\|_{0,\gamma}^2 + \int_{\gamma} \int_{\gamma} \frac{|u(x) - u(y)|^2}{|x - y|^{1+2\sigma}} dx dy \\
&= \|u\|_{0,\gamma}^2 + \int_{\gamma^-} \int_{\gamma^-} \frac{|u(x) - u(y)|^2}{|x - y|^{1+2\sigma}} dx dy + 2 \int_{\gamma^-} \int_{\gamma^+} \frac{|u(x) - u(y)|^2}{|x - y|^{1+2\sigma}} dx dy \\
&\quad + \int_{\gamma^+} \int_{\gamma^+} \frac{|u(x) - u(y)|^2}{|x - y|^{1+2\sigma}} dx dy \\
&\leq \|u\|_{\frac{1}{2},\gamma^-}^2 + \|u\|_{\frac{1}{2},\gamma^+}^2 + C \left(\frac{1}{\epsilon}\right)^{\frac{2(1-\epsilon)}{2-\epsilon}} \left(\|u\|_{\frac{1}{2},\gamma^-}^2 + \|u\|_{\frac{1}{2},\gamma^+}^2\right),
\end{aligned}$$

which leads to

$$\|u\|_{\sigma,\gamma} \leq \frac{C}{\epsilon^{(1-\epsilon)/(2-\epsilon)}} \left(\|u\|_{\frac{1}{2},\gamma^-} + \|u\|_{\frac{1}{2},\gamma^+}\right) \leq \frac{C}{\sqrt{\epsilon}} \left(\|u\|_{\frac{1}{2},\gamma^-} + \|u\|_{\frac{1}{2},\gamma^+}\right)$$

because for small ϵ , we have

$$\frac{1-\epsilon}{2-\epsilon} = \frac{1}{2} - \frac{\epsilon}{4} - \frac{\epsilon^2}{8} - \frac{\epsilon^3}{16} - \dots \leq \frac{1}{2}.$$

□

THEOREM 4.2. *Let $T \in \mathcal{T}_h$ and let γ be an edge of T . Then there exists a constant $C > 0$ such that the following hold on a mesh \mathcal{T}_h with a sufficiently small mesh size:*

1. *If $T \in \mathcal{T}_h^n$ and $v \in H^2(T) + S_h^n(T)$, then*

$$\left\| \beta \frac{\partial v}{\partial \boldsymbol{\nu}} - \Pi_{\boldsymbol{\nu}} v \right\|_{0,\gamma} \leq Ch^{\frac{1}{2}} \|v\|_{H^2(T)}.$$

2. *If $\gamma \in \mathcal{E}_h^n$ but $T \in \mathcal{T}_h^i$, and $v \in \tilde{H}_{\beta}^2(T) + S_h^i(T)$, then*

$$\left\| \beta \frac{\partial v}{\partial \boldsymbol{\nu}} - \Pi_{\boldsymbol{\nu}} v \right\|_{0,\gamma} \leq Ch^{\frac{1}{2}} \left(\|v\|_{H^2(\tilde{T}^-)} + \|v\|_{H^2(\tilde{T}^+)} \right).$$

3. *If $\gamma \in \mathcal{E}_h^i$ and $v \in \tilde{H}_{\beta}^2(T) + S_h^i(T)$, then*

$$\left\| \beta \frac{\partial v}{\partial \boldsymbol{\nu}} - \Pi_{\boldsymbol{\nu}} v \right\|_{0,\gamma} \leq Ch^{\frac{1}{2}} \log h^{\frac{1}{2}} \left(\|v\|_{H^2(\tilde{T}^-)} + \|v\|_{H^2(\tilde{T}^+)} \right).$$

Here, for $T \in \mathcal{T}_h^i$, designate

$$\tilde{T}^s = \begin{cases} T \cap \Omega^s & \text{for } v \in \tilde{H}_{\beta}^2(T), \\ T^s & \text{for } v \in S_h(T), \end{cases} \quad \text{for } s = \pm.$$

Proof. Let $\gamma \in \mathcal{E}_h$. In the first two cases we assume $\gamma \in \mathcal{E}_h^n$, but for the third case we assume $\gamma \in \mathcal{E}_h^i$. Then by the standard trace theorem or the lemma above, we have $\beta \frac{\partial v}{\partial \boldsymbol{\nu}} \in H^{\frac{1}{2}}(\gamma)$ or $\beta \frac{\partial v}{\partial \boldsymbol{\nu}} \in H^{\frac{1}{2}-\epsilon}(\gamma)$ for any $\epsilon \in (0, \frac{1}{4})$.

Since $\Pi_{\boldsymbol{\nu}} v$ is the L^2 projection of $\beta \frac{\partial v}{\partial \boldsymbol{\nu}}$ to the space of constant polynomials, applying the error estimate for polynomial projection and the standard error estimate on interpolation of Sobolev spaces (see [9, Theorem 1.4, p.6]), we have

$$(4.5) \quad \left\| \beta \frac{\partial v}{\partial \boldsymbol{\nu}} - \Pi_{\boldsymbol{\nu}} v \right\|_{0,\gamma} \leq \begin{cases} Ch^{\frac{1}{2}} \left\| \beta \frac{\partial v}{\partial \boldsymbol{\nu}} \right\|_{\frac{1}{2},\gamma} & \text{if } \gamma \in \mathcal{E}_h^n, \\ Ch^{\frac{1}{2}-\epsilon} \left\| \beta \frac{\partial v}{\partial \boldsymbol{\nu}} \right\|_{\frac{1}{2}-\epsilon,\gamma} & \text{if } \gamma \in \mathcal{E}_h^i. \end{cases}$$

For the first two cases, by the definition of $\|\cdot\|_{\frac{1}{2},\gamma}$, we have

$$\left\| \beta \frac{\partial v}{\partial \boldsymbol{\nu}} \right\|_{\frac{1}{2},\gamma} \leq \begin{cases} \left\| \beta \frac{\partial v}{\partial \boldsymbol{\nu}} \right\|_{1,T} & \text{if } T \in \mathcal{T}_h^n, \\ \left\| \beta \frac{\partial v}{\partial \boldsymbol{\nu}} \right\|_{1,\tilde{T}^s} \leq \left\| \beta \frac{\partial v}{\partial \boldsymbol{\nu}} \right\|_{1,\tilde{T}^-} + \left\| \beta \frac{\partial v}{\partial \boldsymbol{\nu}} \right\|_{1,\tilde{T}^+} & \text{if } T \in \mathcal{T}_h^i, \end{cases}$$

which means

$$(4.6) \quad \left\| \beta \frac{\partial v}{\partial \boldsymbol{\nu}} \right\|_{\frac{1}{2},\gamma} \leq \begin{cases} \max\{\beta^+, \beta^-\} \|v\|_{2,T} & \text{if } T \in \mathcal{T}_h^n, \\ \max\{\beta^+, \beta^-\} \|v\|_{\tilde{H}_\beta^2(T)} & \text{if } T \in \mathcal{T}_h^i. \end{cases}$$

For the third case, applying Lemma 4.1, we have

$$(4.7) \quad \begin{aligned} \left\| \beta \frac{\partial v}{\partial \boldsymbol{\nu}} \right\|_{\frac{1}{2}-\epsilon,\gamma} &\leq \frac{C}{\sqrt{\epsilon}} \left(\left\| \beta \frac{\partial v}{\partial \boldsymbol{\nu}} \right\|_{\frac{1}{2},\gamma^-} + \left\| \beta \frac{\partial v}{\partial \boldsymbol{\nu}} \right\|_{\frac{1}{2},\gamma^+} \right) \\ &\leq \frac{C}{\sqrt{\epsilon}} \left(\|v\|_{2,\tilde{T}^-} + \|v\|_{2,\tilde{T}^+} \right). \end{aligned}$$

Finally, all the estimates in this theorem follow by applying (4.6) and (4.7) to (4.5), and by taking the minimum of $\frac{1}{h^\epsilon \sqrt{\epsilon}}$ over $0 < \epsilon < 1/4$. Indeed, at $\epsilon = \frac{1}{2 \log \frac{1}{h}}$, for $0 < h < \frac{1}{e^2}$, the minimum value is

$$\frac{1}{h^\epsilon \sqrt{\epsilon}} = h^{\frac{1}{2 \log h}} \sqrt{2 \log \frac{1}{h}} = \sqrt{2e} |\log h|^{\frac{1}{2}}.$$

□

4.3. The Energy-Norm Error Estimate. Define the (broken) energy norm

$$\| \| u \| \| = \sqrt{a_h(u, u)}.$$

As needed, we quote the following second Strang lemma for the IFE solution:

LEMMA 4.3. *Let $u \in \tilde{H}_\Gamma^1(\Omega)$ and $u_h \in S_h(\Omega)$ be the solutions of (2.1) and (4.1), respectively. Then,*

$$(4.8) \quad \| \| u - u_h \| \| \leq C \left\{ \inf_{v_h \in S_h(\Omega)} \| \| u - v_h \| \| + \sup_{w_h \in S_h(\Omega)} \frac{|a_h(u, w_h) - L(w_h)|}{\| \| w_h \| \|} \right\}.$$

We are now ready to state and derive an error estimate in the energy norm.

THEOREM 4.4. *Let $u \in \tilde{H}_\beta^2(\Omega)$ and $u_h \in S_h(\Omega)$ be the solutions of (2.1) and (4.1), respectively. Then, there exists a constant C such that*

$$(4.9) \quad \| \| u - u_h \| \| \leq Ch \left[\| \| u \|_{\tilde{H}_\beta^2(\Omega)} + |\log h|^{\frac{1}{2}} \sum_{T \in \mathcal{T}_h^i} \| \| u \|_{\tilde{H}_\beta^2(T)} \right].$$

If, in addition, $u \in \tilde{W}_\beta^{2,q}(\Omega)$ for some $q > 2$, then there exists $h_0 > 0$ such that, for all $0 < h < h_0$,

$$(4.10) \quad \| \| u - u_h \| \| \leq Ch \left(\| \| u \|_{\tilde{H}_\beta^2(\Omega)} + \sum_{T \in \mathcal{T}_h^i} \| \| u \|_{\tilde{W}_\beta^{2,q}(T)} \right).$$

Proof. We need to estimate those terms bounding $\|u - u_h\|$ in (4.8) of the Strang lemma above. By the interpolation estimate (3.5), we can estimate the first term on the right hand side of (4.8) as follows:

$$(4.11) \quad \inf_{v_h \in S_h(\Omega)} \|u - v_h\| \leq Ch \|u\|_{\tilde{H}_\beta^2(\Omega)}.$$

Next, let $w_h \in S_h(\Omega)$ be arbitrary. Then, since $u \in H^1(\Omega)$, it follows that

$$\begin{aligned} a_h(u, w_h) &= \sum_j (\beta \nabla u, \nabla w_h)_{T_j} = - \sum_j (\nabla \cdot \beta \nabla u, w_h)_{T_j} + \sum_j \left\langle \beta \frac{\partial u_j}{\partial \boldsymbol{\nu}_j}, w_h \right\rangle_{\partial T_j} \\ &= (-\nabla \cdot \beta \nabla u, w_h) + \sum_j \left\langle \beta \frac{\partial u_j}{\partial \boldsymbol{\nu}_j}, w_h \right\rangle_{\partial T_j}. \end{aligned}$$

Hence, by choosing $m_j \in \mathcal{P}_0(T_j)$ to be the the average of w_h over T_j , one sees that

$$\begin{aligned} a_h(u, w_h) - L(w_h) &= \sum_j \left\langle \beta \frac{\partial u_j}{\partial \boldsymbol{\nu}_j}, w_h \right\rangle_{\partial T_j} = \sum_j \left\langle \beta \frac{\partial u_j}{\partial \boldsymbol{\nu}_j} - \Pi_{\boldsymbol{\nu}} u_j, w_h \right\rangle_{\partial T_j} \\ (4.12) \quad &= \sum_j \left\langle \beta \frac{\partial u_j}{\partial \boldsymbol{\nu}_j} - \Pi_{\boldsymbol{\nu}} u_j, w_h - m_j \right\rangle_{\partial T_j}. \end{aligned}$$

Hence, by Theorem 4.2, the trace inequality on T_j , and the approximation capability of m_j , we have

$$\begin{aligned} &|a_h(u, w_h) - L(w_h)| \\ &\leq \left(\sum_j \left\| \beta \frac{\partial u_j}{\partial \boldsymbol{\nu}_j} - \Pi_{\boldsymbol{\nu}} u_j \right\|_{0, \partial T_j}^2 \right)^{\frac{1}{2}} \left(\sum_j \|w_h - m_j\|_{0, \partial T_j}^2 \right)^{\frac{1}{2}} \\ &\leq \left(Ch^{\frac{1}{2}} \sum_{T \in \mathcal{T}_h^n} \|u\|_{2, T} + Ch^{\frac{1}{2}} |\log h|^{\frac{1}{2}} \sum_{T \in \mathcal{T}_h^i} \|u\|_{\tilde{H}_\beta^2(T)} \right) Ch^{\frac{1}{2}} \left(\sum_j \|\nabla w_h\|_{0, T_j}^2 \right)^{\frac{1}{2}} \\ (4.13) \quad &\leq Ch \left(\sum_{T \in \mathcal{T}_h^n} \|u\|_{2, T} + |\log h|^{\frac{1}{2}} \sum_{T \in \mathcal{T}_h^i} \|u\|_{\tilde{H}_\beta^2(T)} \right) \|w_h\|. \end{aligned}$$

Then, applying (4.11) and (4.13) to (4.8) leads to (4.9).

Assume that $u \in \tilde{W}_\beta^{2, q}(\Omega)$ for some $q > 2$. Then choose p such that $\frac{1}{p} + \frac{2}{q} = 1$, so that, for $T \in \mathcal{T}_h^i$

$$\begin{aligned} \|u\|_{\tilde{H}_\beta^2(T)} &\leq \left(\sum_{s=\pm} \int_{T^s} \sum_{|\alpha| \leq 2} |D^\alpha u|^2 dx \right)^{\frac{1}{2}} \leq \left(\int_T 1^p dx \right)^{\frac{1}{2p}} \left(\sum_{s=\pm} \int_{T^s} \left(\sum_{|\alpha| \leq 2} |D^\alpha u|^2 \right)^{\frac{q}{2}} dx \right)^{\frac{1}{q}} \\ &\leq C |T|^{\frac{1}{2p}} \left(\sum_{s=\pm} \int_{T^s} \sum_{|\alpha| \leq 2} |D^\alpha u|^q dx \right)^{\frac{1}{q}} \leq Ch^{\frac{1}{p}} \|u\|_{\tilde{W}_\beta^{2, q}(T)}. \end{aligned}$$

Hence, the second term in (4.9) can be bounded by

$$|\log h|^{\frac{1}{2}} \sum_{T \in \mathcal{T}_h^i} \|u\|_{\tilde{H}_\beta^2(T)} \leq C \sum_{T \in \mathcal{T}_h^i} |\log h|^{\frac{1}{2}} h^{\frac{1}{p}} \|u\|_{\tilde{W}_\beta^{2, q}(T)}.$$

Since $\lim_{h \rightarrow 0} |\log h|^{\frac{1}{2}} h^{\frac{1}{p}} = 0$, there exists $h_0 > 0$ such that the estimate (4.10) is valid for $0 < h < h_0$. This completes the proof. \square

REMARK 4.1. *Indeed, (4.9) implies that the IFE solution converge faster than $\mathcal{O}(h|\log h|^{\frac{1}{2}})$, since its multiplication factor, $\sum_{T \in \mathcal{T}_h^i} \|u\|_{\tilde{H}_\beta^2(T)}$, goes to zero as $h \rightarrow 0$.*

4.4. Duality and the L^2 -Error Estimate. Let

$$\eta_h = \mathcal{I}_h u - u_h \in \dot{S}_h(\Omega),$$

and let $\psi \in \tilde{H}_\beta^2(\Omega)$ be the solution of the dual problem:

$$(4.14a) \quad -\nabla \cdot (\beta \nabla \psi) = \eta_h \quad \text{in } \Omega,$$

$$(4.14b) \quad \psi = 0 \quad \text{on } \partial\Omega.$$

Assume that the interface problem (2.1) is $\tilde{H}_\beta^2(\Omega)$ -regular so that the elliptic regularity estimate holds:

$$(4.15) \quad \|\psi\|_{\tilde{H}_\beta^2(\Omega)} \leq C \|\eta_h\|_0.$$

We start from recalling the following standard estimates for the IFE interpolation $\mathcal{I}_h \psi$: there exists a constant C such that

$$(4.16) \quad \begin{cases} \|\mathcal{I}_h \psi\|_{2,T} \leq C \|\psi\|_{2,T} & \forall T \in \mathcal{T}_h^n, \\ \|\mathcal{I}_h \psi\|_{2,T_j^-} + \|\mathcal{I}_h \psi\|_{2,T_j^+} \leq C \|\psi\|_{\tilde{H}_\beta^2(T)} & \forall T \in \mathcal{T}_h^i. \end{cases}$$

Since $\eta_h \in \dot{S}_h(\Omega)$, it follows that

$$\begin{aligned} \|\eta_h\|_0^2 &= (-\nabla \cdot \beta \nabla \psi, \eta_h) = a_h(\psi, \eta_h) - \sum_j \left\langle \beta \frac{\partial \psi_j}{\partial \boldsymbol{\nu}_j}, \eta_{h_j} \right\rangle_{\partial T_j} \\ &= a_h(\psi, \eta_h) - \sum_j \left\langle \beta \frac{\partial \psi_j}{\partial \boldsymbol{\nu}_j} - \Pi_{\boldsymbol{\nu}} \psi_j, \eta_{h_j} - q_j \right\rangle_{\partial T_j} \quad \text{for all } q_j \in \mathcal{P}_0(T_j). \end{aligned}$$

Next, for all $v_h \in \dot{S}_h(\Omega)$, similarly to (4.12), we have

$$\begin{aligned} a_h(\eta_h, v_h) &= a_h(u, v_h) - a_h(u_h, v_h) - a_h(u - \mathcal{I}_h u, v_h) \\ &= \sum_j \left\langle \beta \frac{\partial u_j}{\partial \boldsymbol{\nu}_j} - \Pi_{\boldsymbol{\nu}} u_j, v_{h_j} \right\rangle_{\partial T_j} - a_h(u - \mathcal{I}_h u, v_h). \end{aligned}$$

Using the property $[\psi]_{\gamma_{jk}} = 0$ and recalling the definition of $\Pi_{\boldsymbol{\nu}}$, we see that

$$\left\langle \beta \frac{\partial u_j}{\partial \boldsymbol{\nu}_j} - \Pi_{\boldsymbol{\nu}} u_j, \psi_j \right\rangle_{\gamma_{jk}} + \left\langle \beta \frac{\partial u_k}{\partial \boldsymbol{\nu}_k} - \Pi_{\boldsymbol{\nu}} u_k, \psi_k \right\rangle_{\gamma_{kj}} = 0.$$

In addition, note that for $v_h \in S_h(\Omega)$, $-\nabla \cdot (\beta \nabla v_h) = 0$ on every $T \in \mathcal{T}_h$; hence,

$$\begin{aligned} a_h(u - \mathcal{I}_h u, v_h) &= \sum_j (u - \mathcal{I}_h u, -\nabla \cdot (\beta \nabla v_h))_{T_j} + \sum_j \left\langle u - \mathcal{I}_h u, \beta \frac{\partial v_h}{\partial \boldsymbol{\nu}_j} \right\rangle_{\partial T_j} \\ &= \sum_j \left\langle u - \mathcal{I}_h u, \beta \frac{\partial v_h}{\partial \boldsymbol{\nu}_j} - \Pi_{\boldsymbol{\nu}_j} v_h \right\rangle_{\partial T_j}. \end{aligned}$$

Therefore

$$\begin{aligned}
\|\eta_h\|_0^2 &= a_h(\psi, \eta_h) - \sum_j \left\langle \beta \frac{\partial \psi_j}{\partial \boldsymbol{\nu}_j} - \Pi_{\boldsymbol{\nu}} \psi_j, \eta_{h_j} - q_j \right\rangle_{\partial T_j} \\
&= a_h(\eta_h, \psi - v_h) - a_h(u - \mathcal{I}_h u, v_h) \\
&\quad - \sum_j \left\langle \beta \frac{\partial \psi_j}{\partial \boldsymbol{\nu}_j} - \Pi_{\boldsymbol{\nu}} \psi_j, \eta_{h_j} - q_j \right\rangle_{\partial T_j} + \sum_j \left\langle \beta \frac{\partial u_j}{\partial \boldsymbol{\nu}_j} - \Pi_{\boldsymbol{\nu}} u_j, v_{h_j} - \psi_j \right\rangle_{\partial T_j} \\
&= a_h(\eta_h, \psi - v_h) - \sum_j \left\langle u - \mathcal{I}_h u, \beta \frac{\partial v_h}{\partial \boldsymbol{\nu}_j} - \Pi_{\boldsymbol{\nu}_j} v_h \right\rangle_{\partial T_j} \\
(4.17) \quad &- \sum_j \left\langle \beta \frac{\partial \psi_j}{\partial \boldsymbol{\nu}_j} - \Pi_{\boldsymbol{\nu}} \psi_j, \eta_{h_j} - q_j \right\rangle_{\partial T_j} + \sum_j \left\langle \beta \frac{\partial u_j}{\partial \boldsymbol{\nu}_j} - \Pi_{\boldsymbol{\nu}} u_j, v_{h_j} - \psi_j \right\rangle_{\partial T_j}.
\end{aligned}$$

With these preparations, we are ready to derive the error estimate in the L^2 -norm for the IFE solution.

THEOREM 4.5. *Assume the interface problem (2.1) is $\tilde{H}_\beta^2(\Omega)$ -regular. Then, there exists a constant C such that the L^2 -norm error of the IFE solution satisfies the following estimate:*

$$(4.18) \quad \|u - u_h\|_0 \leq Ch^2 \left[|\log h|^{\frac{1}{2}} \|u\|_{\tilde{H}_\beta^2(\Omega)} + |\log h| \sum_{T \in \mathcal{T}_h^i} \|u\|_{\tilde{H}_\beta^2(T)} \right].$$

Proof. We proceed to estimate each term on the right hand side of (4.17). First, choose $v_h = \mathcal{I}_h \psi$. Then, by (3.5) and (4.15), the first term on the right-hand side of (4.17) is bounded as follows:

$$(4.19) \quad |a_h(\eta_h, \psi - v_h)| = |a_h(\eta_h, \psi - \mathcal{I}_h \psi)| \leq Ch \|\eta_h\| \|\eta_h\|_0.$$

Again, choosing $q_j \in \mathcal{P}_0(T_j)$ to be the the average of η_h over T_j , by Theorem 4.2, the trace inequality on T_j , Theorem 3.2, and (4.15), we can bound the last two terms on the right hand side of (4.17) as follows:

$$\begin{aligned}
&\left| \sum_j \left\langle \beta \frac{\partial \psi_j}{\partial \boldsymbol{\nu}_j} - \Pi_{\boldsymbol{\nu}} \psi_j, \eta_{h_j} - q_j \right\rangle_{\partial T_j} \right| + \left| \sum_j \left\langle \beta \frac{\partial u_j}{\partial \boldsymbol{\nu}_j} - \Pi_{\boldsymbol{\nu}} u_j, v_{h_j} - \psi_j \right\rangle_{\partial T_j} \right| \\
&\leq Ch \left(\sum_{T \in \mathcal{T}_h^n} \|\psi\|_{2,T} + |\log h|^{\frac{1}{2}} \sum_{T \in \mathcal{T}_h^i} \|\psi\|_{\tilde{H}_\beta^2(T)} \right) \|\eta_h\| \\
&\quad + Ch^2 \left(\sum_{T \in \mathcal{T}_h^n} \|u\|_{2,T} + |\log h|^{\frac{1}{2}} \sum_{T \in \mathcal{T}_h^i} \|u\|_{\tilde{H}_\beta^2(T)} \right) \|\psi\|_{\tilde{H}_\beta^2(\Omega)} \\
(4.20) \quad &\leq Ch \left(|\log h|^{\frac{1}{2}} \|\eta_h\| + h \sum_{T \in \mathcal{T}_h^n} \|u\|_{2,T} + h |\log h|^{\frac{1}{2}} \sum_{T \in \mathcal{T}_h^i} \|u\|_{\tilde{H}_\beta^2(T)} \right) \|\eta_h\|_0.
\end{aligned}$$

For the second term in (4.17), by Theorem 3.2, Theorem 4.2, (4.16) and (4.15),

$$\begin{aligned}
& \left| \sum_j \left\langle u - \mathcal{I}_h u, \beta \frac{\partial v_{h_j}}{\partial \boldsymbol{\nu}_j} - \Pi_{\boldsymbol{\nu}_j} v_h \right\rangle_{\partial T_j} \right| \\
& \leq \left(\sum_j |u - \mathcal{I}_h u|_{0, \partial T_j}^2 \right)^{\frac{1}{2}} \left(\sum_j \left| \beta \frac{\partial v_{h_j}}{\partial \boldsymbol{\nu}_j} - \Pi_{\boldsymbol{\nu}_j} v_h \right|_{0, \partial T_j}^2 \right)^{\frac{1}{2}} \\
& \leq Ch^{\frac{3}{2}} \|u\|_{\tilde{H}_\beta^2(\Omega)} \left(h \sum_{T \in \mathcal{T}_h^n} \|v_h\|_{\tilde{H}_\beta^2(T)}^2 + h |\log h| \sum_{T \in \mathcal{T}_h^i} (\|v_h\|_{2, T^-}^2 + \|v_h\|_{2, T^+}^2) \right)^{\frac{1}{2}} \\
(4.21) \quad & \leq Ch^2 |\log h|^{\frac{1}{2}} \|u\|_{\tilde{H}_\beta^2(\Omega)} \|\eta_h\|_0.
\end{aligned}$$

Plugging the estimates (4.19)–(4.21) in (4.17) gives

$$\begin{aligned}
\|\eta_h\|_0 & \leq Ch |\log h|^{\frac{1}{2}} \|\eta_h\| + Ch^2 |\log h|^{\frac{1}{2}} \|u\|_{\tilde{H}_\beta^2(\Omega)} \\
& \leq Ch |\log h|^{\frac{1}{2}} (\|\mathcal{I}_h u - u\| + \|u - u_h\|) + Ch^2 |\log h|^{\frac{1}{2}} \|u\|_{\tilde{H}_\beta^2(\Omega)}.
\end{aligned}$$

Finally, applying Theorem 3.2 and Theorem 4.4 to the above estimate, we arrive at the desired estimate (4.18). This completes the proof. \square

REMARK 4.2. *The estimate given in (4.18) suggests that the IFE solution converges in L^2 -norm better than $\mathcal{O}(h^2 |\log h|)$ which is optimal sans the usual $|\log h|$ factor.*

REMARK 4.3. *An optimal rate $\mathcal{O}(h^2)$ without $|\log h|$ factor may be obtained with slightly better regularity $u \in \tilde{W}_\beta^{2,q}(\Omega)$, $q > 2$, and the elliptic regularity assumption based on L^q -norm. In addition, the analysis requires the interpolation error estimates for IFE functions based on L^q -norm, which will be an interesting future work.*

5. Numerical Examples. In this section, we present numerical examples to demonstrate the features of this nonconforming rotated- Q_1 IFE method for elliptic interface problems.

We test these IFE methods with the same example as given in [14, 31]. Let $\Omega = (-1, 1)^2$, and the interface curve Γ is the circle centered at the origin with radius $r_0 = \pi/6.28$, which separates the domain into two sub-domains:

$$\Omega^- = \{(x, y) \in \Omega : x^2 + y^2 < r_0^2\}, \quad \Omega^+ = \{(x, y) \in \Omega : x^2 + y^2 > r_0^2\}.$$

The boundary condition g and the source function f are chosen such that the exact solution is as follows:

$$(5.1) \quad u(x, y) = \begin{cases} \frac{r^a}{\beta^-} & \text{if } r < r_0, \\ \frac{r^a}{\beta^+} + \left(\frac{1}{\beta^-} - \frac{1}{\beta^+} \right) r_0^a & \text{if } r > r_0, \end{cases}$$

where $a = 5$, $r = \sqrt{x^2 + y^2}$. We use a family of Cartesian meshes $(\mathcal{T}_h)_{0 < h < 1}$, each of which consists of $N \times N$ congruent squares of size $h = 2/N$. Errors of an IFE approximation are given in L^∞ -, L^2 -, and semi H^1 - norms. Error in L^∞ -norm is calculated using the formula:

$$(5.2) \quad \|u_h - u\|_{L^\infty} = \max_{T \in \mathcal{T}_h} \left(\max_{(x,y) \in \hat{T} \subset T} |u_h(x, y) - u(x, y)| \right),$$

where \hat{T} consists of the 49 uniformly distributed points in T . The L^2 and semi H^1 norms are computed using the 9-point Gaussian quadratures.

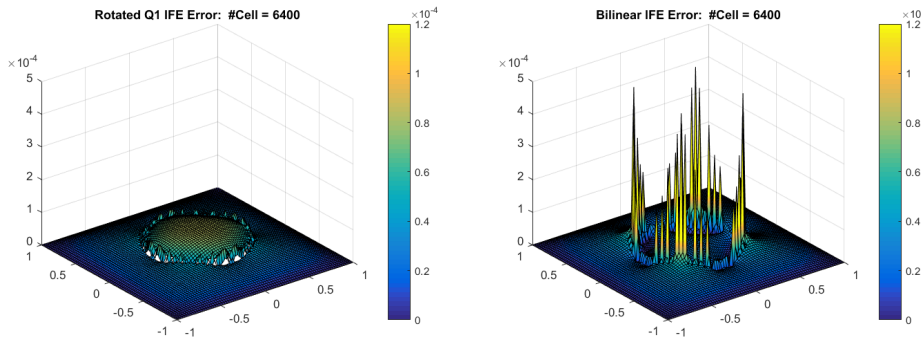
Our first numerical experiment considers a moderate coefficient jump $(\beta^-, \beta^+) = (1, 10)$. Errors of numerical solutions are reported in Table 5.1. Convergence rates in semi H^1 -norm and L^2 -norm confirm our error analysis (4.9) and (4.18). Data in these tables also suggest that the convergence rate in L^∞ -norm are approximately $O(h^2)$, which is also optimal from the point view of the degree of polynomials in constructing IFE spaces $S_h(\Omega)$.

TABLE 5.1
Errors of Galerkin IFE solutions $u - u_h$ with $\beta^- = 1, \beta^+ = 10$

N	$\ \cdot\ _{L^\infty}$	rate	$\ \cdot\ _{L^2}$	rate	$ \cdot _{H^1}$	rate
10	$2.6183E-2$		$1.1395E-2$		$1.9585E-1$	
20	$7.3444E-3$	1.8339	$2.9860E-3$	1.9321	$9.9065E-2$	0.9833
40	$1.9455E-3$	1.9165	$7.4374E-4$	2.0054	$4.9894E-2$	0.9895
80	$5.0072E-4$	1.9580	$1.8547E-4$	2.0036	$2.5026E-2$	0.9955
160	$1.2702E-4$	1.9789	$4.6313E-5$	2.0017	$1.2531E-2$	0.9979
320	$3.1989E-5$	1.9894	$1.1671E-5$	1.9885	$6.2702E-3$	0.9990
640	$8.0267E-6$	1.9947	$2.9122E-6$	2.0027	$3.1363E-3$	0.9995
1280	$2.0101E-6$	1.9975	$7.2684E-7$	2.0024	$1.5684E-3$	0.9997

The error surface $e_h = |u_h - u|$ are reported in Figure 5.1. For comparison, we also plot the error surface of Lagrange bilinear IFE solutions [14, 15]. These plots are generated on the same mesh containing 80×80 elements. We note that the error of bilinear IFE solution is much larger around interface than the rest of domain, in fact, the error at the interface looks like an “interface crown”. However, the nonconforming IFE solution is much more accurate than bilinear IFE solution around the interface. In fact, there is no apparent “crown” around interface, which indicates the accuracy of nonconforming IFE solution around interface are comparable to the accuracy far away from the interface.

FIG. 5.1. Comparison of point-wise errors of the nonconforming rotated Q_1 IFE and the bilinear IFE solutions



Next, we take a closer look of the nonconforming rotated- Q_1 IFE functions and Lagrange bilinear IFE functions [14]. In Figure 5.2, we plot the global bases of bilinear and rotated- Q_1 IFE function on two adjacent elements. In the left plot, there is a large gap on common interface edge of a bilinear IFE basis, where the continuity is only enforced at two endpoints of that edge. To see it more clearly, in the right plot,

the traces of this bilinear IFE function are plotted in blue curves which indicate that the largest discontinuity occurs at the intersection point of the edge and the interface. On the other hand, the middle plot shows that the discontinuity of a rotated- Q_1 IFE basis is scattered throughout the interface edge and it is less prominent. In fact, the rotated- Q_1 basis is weakly continuous across the edge in the sense that the mean values of the two traces are exactly the same. The traces of this rotated- Q_1 IFE function are plotted in red curves which also demonstrate a smaller discontinuity across the interface edge. This shows why the rotated Q_1 IFE methods outperform bilinear IFE methods.

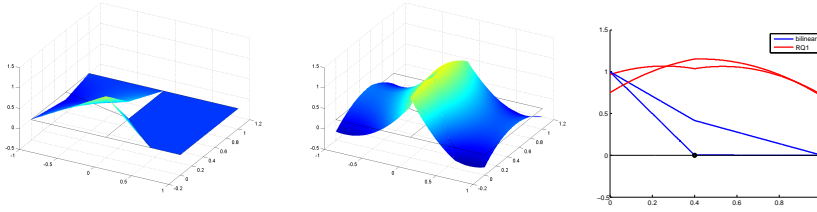


FIG. 5.2. Comparison of bilinear and rotated- Q_1 IFE global bases with $\beta^- = 1$, $\beta^+ = 1000$.

As for robustness of our nonconforming IFE methods respect to the contrast of jumping coefficient, we test our methods in additional three coefficient configurations including the large contrast $(\beta^-, \beta^+) = (1, 10000)$, the flipping of the coefficients, i.e., $(\beta^-, \beta^+) = (10, 1)$, and $(\beta^-, \beta^+) = (10000, 1)$. Errors and convergence rates are reported in Tables 5.2, 5.3, and 5.4, respectively. The convergence rates for all the cases are optimal, and this suggests the robustness of our IFE scheme with respect to the jump of coefficients.

TABLE 5.2
Errors of Galerkin IFE solutions $u - u_h$ with $\beta^- = 1$, $\beta^+ = 10000$

N	$\ \cdot\ _{L^\infty}$	rate	$\ \cdot\ _{L^2}$	rate	$ \cdot _{H^1}$	rate
10	$5.9646E-3$		$2.7360E-3$		$4.0678E-2$	
20	$2.5455E-3$	1.2285	$1.0526E-3$	1.3782	$2.7824E-2$	0.5479
40	$7.1692E-4$	1.8281	$2.5767E-4$	2.0303	$1.4700E-2$	0.9205
80	$2.1533E-4$	1.7353	$6.3614E-5$	2.0181	$7.5491E-3$	0.9614
160	$5.9653E-5$	1.8519	$1.5531E-5$	2.0342	$3.7978E-3$	0.9911
320	$1.5521E-5$	1.9423	$4.0823E-6$	1.9277	$1.9146E-3$	0.9881
640	$4.1575E-6$	1.9005	$1.0069E-6$	2.0194	$9.5881E-4$	0.9977
1280	$1.0588E-6$	1.9733	$2.4921E-7$	2.0145	$4.8004E-4$	0.9981

6. Conclusions. In this article, we develop the rotated- Q_1 nonconforming IFE space based on integral value degrees of freedom. This new IFE space can be used in the usual Galerkin formulation to solve elliptic interface problems. The IFE space is proved to have optimal approximation capabilities. Error analysis of the Galerkin IFE solutions using integral-value degrees of freedom shows the quasi-optimal convergence rates in both energy and the L^2 norms.

TABLE 5.3
 Errors of Galerkin IFE solutions $u - u_h$ with $\beta^- = 10$, $\beta^+ = 1$

N	$\ \cdot\ _{L^\infty}$	rate	$\ \cdot\ _{L^2}$	rate	$ \cdot _{H^1}$	rate
10	$2.5249E-2$		$1.0347E-1$		$1.8872E-0$	
20	$6.1647E-3$	2.0341	$2.6094E-2$	1.9874	$9.5266E-1$	0.9862
40	$1.5899E-3$	1.9551	$6.5402E-3$	1.9963	$4.7745E-1$	0.9966
80	$4.0597E-4$	1.9695	$1.6363E-3$	1.9989	$2.3887E-1$	0.9991
160	$1.0382E-4$	1.9673	$4.0917E-4$	1.9997	$1.1945E-1$	0.9998
320	$2.6221E-5$	1.9853	$1.0227E-4$	2.0003	$5.9730E-2$	0.9999
640	$6.6006E-6$	1.9900	$2.5570E-5$	1.9998	$2.9865E-2$	1.0000
1280	$1.6613E-6$	1.9903	$6.3931E-6$	1.9999	$1.4933E-2$	1.0000

TABLE 5.4
 Errors of Galerkin IFE solutions $u - u_h$ with $\beta^- = 10000$, $\beta^+ = 1$

N	$\ \cdot\ _{L^\infty}$	rate	$\ \cdot\ _{L^2}$	rate	$ \cdot _{H^1}$	rate
10	$2.5887E-2$		$1.0332E-1$		$1.8874E-0$	
20	$9.0928E-3$	1.5094	$2.6085E-2$	1.9858	$9.5275E-1$	0.9862
40	$2.2570E-3$	2.0144	$6.5319E-3$	1.9977	$4.7747E-1$	0.9967
80	$5.1846E-4$	2.1180	$1.6345E-3$	1.9987	$2.3887E-1$	0.9992
160	$1.3253E-4$	1.9679	$4.0880E-4$	1.9994	$1.1945E-1$	0.9998
320	$3.1459E-5$	2.0748	$1.0219E-4$	2.0002	$5.9729E-2$	0.9999
640	$7.7833E-6$	2.0150	$2.5551E-5$	1.9998	$2.9865E-2$	1.0000
1280	$1.9252E-6$	2.1504	$6.3885E-6$	1.9998	$1.4933E-2$	1.0000

- [1] I. Babuška. The finite element method for elliptic equations with discontinuous coefficients. *Computing (Arch. Elektron. Rechnen)*, 5:207–213, 1970.
- [2] W. Cao, X. Zhang, and Z. Zhang. Superconvergence of immersed finite element methods for interface problems. *Adv. Comput. Math.*, 43(4):795–821, 2017.
- [3] Z. Chen and P. Oswald. Multigrid and multilevel methods for nonconforming Q_1 elements. *Math. Comp.*, 67(222):667–693, 1998.
- [4] Z. Chen and J. Zou. Finite element methods and their convergence for elliptic and parabolic interface problems. *Numer. Math.*, 79(2):175–202, 1998.
- [5] S.-H. Chou, D. Y. Kwak, and K. T. Wee. Optimal convergence analysis of an immersed interface finite element method. *Adv. Comput. Math.*, 33(2):149–168, 2010.
- [6] P. G. Ciarlet. *The finite element method for elliptic problems*. North-Holland Publishing Co., Amsterdam-New York-Oxford, 1978. Studies in Mathematics and its Applications, Vol. 4.
- [7] M. Crouzeix and P.-A. Raviart. Conforming and nonconforming finite element methods for solving the stationary Stokes equations. I. *Rev. Française Automat. Informat. Recherche Opérationnelle Sér. Rouge*, 7(R-3):33–75, 1973.
- [8] J. Douglas, Jr., J. E. Santos, D. Sheen, and X. Ye. Nonconforming Galerkin methods based on quadrilateral elements for second order elliptic problems. *M2AN Math. Model. Numer. Anal.*, 33(4):747–770, 1999.
- [9] V. Girault and P.-A. Raviart. *Finite element methods for Navier-Stokes equations*, volume 5 of *Springer Series in Computational Mathematics*. Springer-Verlag, Berlin, 1986. Theory and algorithms.
- [10] Y. Gong, B. Li, and Z. Li. Immersed-interface finite-element methods for elliptic interface problems with nonhomogeneous jump conditions. *SIAM J. Numer. Anal.*, 46(1):472–495, 2007/08.
- [11] R. Guo and T. Lin. A group of immersed finite element spaces for elliptic interface problems. *arXiv:1612.00919*, 2016.
- [12] R. Guo, T. Lin, and X. Zhang. Nonconforming Immersed Finite Element Spaces for Elliptic Interface Problems. *arXiv:1612.01862*, 2016.
- [13] J. Guzmán, M. A. Sánchez, and M. Sarkis. A finite element method for high-contrast interface problems with error estimates independent of contrast. *J. Sci. Comput.*, 73(1):330–365,

- 2017.
- [14] X. He, T. Lin, and Y. Lin. Approximation capability of a bilinear immersed finite element space. *Numer. Methods Partial Differential Equations*, 24(5):1265–1300, 2008.
 - [15] X. He, T. Lin, and Y. Lin. The convergence of the bilinear and linear immersed finite element solutions to interface problems. *Numer. Methods Partial Differential Equations*, 28(1):312–330, 2012.
 - [16] X. He, T. Lin, Y. Lin, and X. Zhang. Immersed finite element methods for parabolic equations with moving interface. *Numer. Methods Partial Differential Equations*, 29(2):619–646, 2013.
 - [17] Y. Jeon, H. Nam, D. Sheen, and K. Shim. A class of nonparametric DSSY nonconforming quadrilateral elements. *ESAIM Math. Model. Numer. Anal.*, 47(6):1783–1796, 2013.
 - [18] H. Ji, J. Chen, and Z. Li. A symmetric and consistent immersed finite element method for interface problems. *J. Sci. Comput.*, 61(3):533–557, 2014.
 - [19] R. Kafafy, T. Lin, Y. Lin, and J. Wang. Three-dimensional immersed finite element methods for electric field simulation in composite materials. *Internat. J. Numer. Methods Engrg.*, 64(7):940–972, 2005.
 - [20] R. Kafafy and J. Wang. Whole ion optics gridlet simulations using a hybrid-grid immersed-finite-element particle-in-cell code. *J. Propulsion Power*, 23(1):59–68, 2007.
 - [21] P. Klouček, B. Li, and M. Luskin. Analysis of a class of nonconforming finite elements for crystalline microstructures. *Math. Comp.*, 65(215):1111–1135, 1996.
 - [22] D. Y. Kwak, K. T. Wee, and K. S. Chang. An analysis of a broken P_1 -nonconforming finite element method for interface problems. *SIAM J. Numer. Anal.*, 48(6):2117–2134, 2010.
 - [23] Z. Li, T. Lin, Y. Lin, and R. C. Rogers. An immersed finite element space and its approximation capability. *Numer. Methods Partial Differential Equations*, 20(3):338–367, 2004.
 - [24] Z. Li, T. Lin, and X. Wu. New Cartesian grid methods for interface problems using the finite element formulation. *Numer. Math.*, 96(1):61–98, 2003.
 - [25] T. Lin, Y. Lin, and X. Zhang. A method of lines based on immersed finite elements for parabolic moving interface problems. *Adv. Appl. Math. Mech.*, 5(4):548–568, 2013.
 - [26] T. Lin, Y. Lin, and X. Zhang. Partially penalized immersed finite element methods for elliptic interface problems. *SIAM J. Numer. Anal.*, 53(2):1121–1144, 2015.
 - [27] T. Lin, D. Sheen, and X. Zhang. A locking-free immersed finite element method for planar elasticity interface problems. *J. Comput. Phys.*, 247:228–247, 2013.
 - [28] T. Lin, Q. Yang, and X. Zhang. *A Priori* error estimates for some discontinuous Galerkin immersed finite element methods. *J. Sci. Comput.*, 65(3):875–894, 2015.
 - [29] R. Rannacher and S. Turek. Simple nonconforming quadrilateral Stokes element. *Numer. Methods Partial Differential Equations*, 8(2):97–111, 1992.
 - [30] S. Vallaghé and T. Papadopoulos. A trilinear immersed finite element method for solving the electroencephalography forward problem. *SIAM J. Sci. Comput.*, 32(4):2379–2394, 2010.
 - [31] X. Zhang. *Nonconforming Immersed Finite Element Methods for Interface Problems*. 2013. Thesis (Ph.D.)—Virginia Polytechnic Institute and State University.